

Dianion Stabilization by $(M(C_5(CH_3)_5)_2)^+$: Theoretical Evidence for a Localized Ring in $(DDQ)^{2-}$

JOEL S. MILLER AND DAVID A. DIXON

Organic dianions have been stabilized by $(M(C_5(CH_3)_5)_2)^+$, where M is iron or cobalt. This has allowed the structural and spectroscopic characterization of these dianions. The structure of $(M(C_5(CH_3)_5)_2)^+(DDQ)^{2-}$, where DDQ is 2,3-dichloro-5,6-dicyanobenzoquinone, has been determined by x-ray crystallography. The structure of $(DDQ)^{2-}$ is consistent with ab initio molecular orbital calculations that suggest a localized as opposed to a delocalized (aromatic) ring structure.

CERTAIN ORGANOMETALLIC CHARGE-transfer complexes are of interest in that they exhibit cooperative magnetic phenomena (1-4), for example, meta- and ferromagnetism. We have prepared a broad new class of charge-transfer compounds that consist of repeated units of donors (D) and acceptors (A) of the form DAD. The donors and acceptors have reversible redox couples of one and two electrons, respectively. Examples of such complexes for which we have supportive elemental analysis include $(M(C_5(CH_3)_5)_2)_2A$ [where M = Fe; A = $C_4(CN)_6$, $C_6(CN)_6$, or TCNQF₄; and where M = Co; A = TCNQ, TCNQF₄, DDQ, $C_6(CN)_6$, or $C_4(CN)_6$] (5). For a given acceptor, the iron and cobalt complexes, in the cases where they were characterized by single-crystal x-ray diffraction, were found to be isomorphous. However, the space group was dependent on the anion. Several possible assignments for the oxidation states are plausible, such as $\cdots D^+A^{2-}D^+ \cdots$ (1), $\cdots D^+A^{1-}D^0 \cdots \equiv \cdots D^0A^{1-}D^+ \cdots$ (2), and $\cdots D^{1/2+}A^{1-}D^{1/2+} \cdots$ (3). However, the iron complexes exhibited ⁵⁷Fe Mossbauer quadrupole splitting and isomer shifts that are consistent with an Fe(III) species (6). In the structures that were determined, iron or cobalt atoms were crystallographically equivalent. Thus, structure 1 with a dianion (A^{2-}) is the best description for this general class of compounds. The 2:1 complex DAD is black. This is

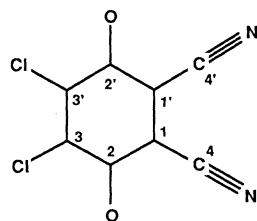
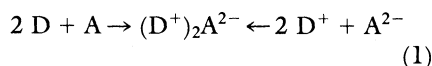


Fig. 1. Labeling of atoms for $(DDQ)^n$.

surprising, because $(Fe(C_5(CH_3)_5)_2)^+$ and $(Co(C_5(CH_3)_5)_2)^+$ are light green and yellow, respectively, and the closed shell dianion is expected to be yellow or light red. This general method of stabilizing organic dianions for their structural and spectroscopic characterization can be represented as:



An example of a charge-transfer salt that was studied by x-ray diffraction is $(Co(C_5(CH_3)_5)_2)_2(DDQ)$ (7). The structure of $(DDQ)^{2-}$ is shown in Fig. 1. The bond distances for the planar dianion are listed in Table 1. Reduction of $(DDQ)^n$ from the neutral species ($n = 0$) to the dianion ($n = -2$) leads to an increase in the C-O and central $C_1-C_{1'}$ bond lengths; however, the C_1-C_2 bond length decreases.

We have performed ab initio molecular orbital calculations on neutral and anionic organic acceptors to obtain structural (geometry optimization), spectral (force field), and electronic (wave function) information (8-10). Such calculations are useful for examining trends in the isolated ions and are especially helpful when disorder, as observed for $(DDQ)^{2-}$, occurs.

The structure of the dianion should establish the anionic charge. However, $(DDQ)^{2-}$ in these crystals is disordered; therefore, spectroscopic and computational methods must be used as well. Examination of the $(Co(C_5(CH_3)_5)_2)^+$ structure shows an average Co-C distance (R_{MC}) of 2.045 (± 0.010) Å and an average Co-C₅ ring centroid distance (R_{MRC}) of 1.655 (± 0.003) Å. The isoelectronic Fe(II) compound has essentially the same values ($R_{MC} = 2.050$ Å; $R_{MRC} = 1.656$ Å) (11). The Fe(III) complex $(Fe(C_5(CH_3)_5)_2)^+$ has significantly larger values for R_{MRC} (1.703 Å) and R_{MC} (2.092 Å) (2). On the basis of

this trend, the unknown R_{MC} and R_{MRC} values for $Co(C_5(CH_3)_5)_2$ should be ~ 0.04 Å shorter than those for the Co(III) complex $Co(C_5(CH_3)_5)_2^+$. Since both cations are equivalent, we conclude that both cobalt atoms are Co(III). Thus the acceptor must be a dianion to conserve charge.

The calculations were performed with the minimal STO-3G basis set (12) and the HONDO (13) and GRADSCF (14) programs. Geometries were gradient-optimized (15, 16) [restricted Hartree-Fock (RHF) for the $n = 0$ and -2 closed-shell species and unrestricted Hartree-Fock (UHF) for the $n = -1$ open-shell radical anion]. Force fields for the closed-shell species were determined analytically (17). The calculated structures for DDQ and $(DDQ)^-$ were taken from earlier work (9) and are in good agreement with the experimental values, except for $r(C-Cl)$ and $r(C=O)$. The calculated distances for these bonds were too long for the $n = -1$ case. The large value for $r(C-Cl)$ is caused by the use of the minimal STO-3G basis set. The use of the UHF wave function, as opposed to an RHF wave function, caused the difference in $r(C-O)$ values for the $n = -1$ case.

For $(DDQ)^{2-}$ the calculated value for $r(C=O)$ is 0.04 Å greater than the value in DDQ and is within 0.01 Å of the experimental value for $(DDQ)^{2-}$. The value for $r(C_1-C_{1'})$ increased from 1.334 Å in DDQ to 1.470 Å in $(DDQ)^{2-}$, while $r(C_1-C_2)$ decreased from 1.522 to 1.420 Å. The C_2-C_3 and C_3-C_3' bonds were essentially unchanged and only small changes were found in the cyano moiety. These results indicate a localized structure in the ring as opposed to a completely delocalized aromatic structure. The structure resembles a substituted ethylene group ($ClC=CCl$) bonded to a group that is similar to a delocalized 1,3-butadiene group; that is, $C_1-C_{1'}$ is a single bond. The electron density from the C_1-C_2 "double bond" delocalized into the cyano group [$r(C_1-C_4)$ decreased] and also into the oxygen atoms, which caused the C-O bond to be shorter than a normal C-O single bond distance of 1.43 Å (18, 19).

In order to demonstrate that the localized structure for $(DDQ)^{2-}$ is not an effect due to our use of a minimal basis set, we optimized the structure for $(DDQ)^{2-}$ with a much larger basis set (20) on a Cray-1A computer. This basis set is of double zeta quality in the valence space on all atoms (21) and is augmented by a set of *d* functions (exponent = 0.70) on the chlorine atoms. The C_2-O bond length increased by 0.032 Å, while the C_3-Cl bond length decreased

Central Research and Development Department, Experimental Station, E. I. du Pont de Nemours and Company, Wilmington, DE 19898.

Table 1. Summary of the bond distances for neutral and anionic DDQ species. The chloride and cyano groups are disordered in DDQ²⁻. Abbreviations: Expt, experimental values; Calc, calculated values.

Bond	Bond length (Å)						
	DDQ		DDQ ⁻		DDQ ²⁻		
	Expt*	Calc-3G†	Expt*	Calc-3G†	Expt	Calc-3G†	Calc-DZD‡
r(C ₂ -O)	1.208	1.222	1.247	1.310	1.25(1)	1.262	1.295
r(C ₁ -C ₂)	1.496	1.522	1.444	1.445	1.43(1)	1.420	1.405
r(C ₂ -C ₃)	1.483	1.520	1.459	1.481	1.43(1)	1.515	1.463
r(C ₁ -C _{1'})	1.341	1.334	1.385	1.386	1.39(1)	1.470	1.450
r(C ₃ -C _{3'})	1.344	1.344	1.360	1.340	1.39(1)	1.341	1.366
r(C ₃ -Cl)	1.715	1.768	1.724	1.789		1.816	1.795
r(C ₁ -C ₄)	1.455	1.458	1.434	1.454		1.432	1.430
r(C ₄ -N)	1.135	1.158	1.120	1.163		1.163	1.161

*Data taken from (9). †Calculated with a STO-3G basis set. ‡Calculated with a double zeta basis set augmented by a set of *d* functions on the chlorine atoms.

by 0.021 Å, as compared to the STO-3G results (see Table 1). The C-C and C≡N bond lengths for the cyano groups were unchanged. The bond lengths in the ring show that a localized structure persists with the larger basis set, although the effect is not as pronounced as with the smaller basis set. For example, the C₃-C_{3'} double bond length increased by 0.025 Å, and the C₂-C₃ single bond length decreased by 0.05 Å. However, the C₂-C₃ single bond is only 0.019 Å shorter than the *sp*²-*sp*² single bond calculated for *cis*-1,3-butadiene (22) with this level of basis set. Bond alternation is still observed, and the C₃-C_{3'} bond is still essentially a double bond.

The experimental values for (DDQ)²⁻ in Table 1 are averages due to the intrinsic crystallographic disorder. We obtain a value of 1.468 Å for the average of the bond distances r(C₁-C₂) and r(C₂-C₃) calculated with the STO-3G basis set, as compared to 1.43 (± 0.01) Å from experiment. The average calculated value for r(C₁-C_{1'}) and r(C₃-C_{3'}) is 1.406 Å, which agrees with the experimental value of 1.39 (± 0.01) Å. The average calculated values are in good agreement with the experimental values if the

agreement of 0.02 to 0.03 Å obtained for DDQ and (DDQ)⁻ is considered. Even better agreement is found for the average values when the larger basis set is employed; 1.434 Å (calculated) versus 1.43 (± 0.01) Å (experimental), and 1.408 Å (calculated) versus 1.39 (± 0.01) Å (experimental). Without the theoretical results, the experimental values would lead us to the conclusion that the C₆ ring is more aromatic than is actually the case.

In addition to the structure for (DDQ)²⁻, the structures of (TCNQ)²⁻, (TCNQF₄)²⁻, (TCNE)²⁻, (TCNQ(CN)₄)²⁻, (C₄(CN)₆)²⁻ and (C₆(CN)₆)²⁻ were determined and their vibrational spectra were obtained. Non-planar structures have been refined for (TCNQF₄)²⁻, (TCNQ(CN)₄)²⁻, and (TCNE)²⁻ (23). As anticipated, reduction to the dianion weakens the C≡N bond, which shifts the vibrational frequency to lower values (see Table 2). The experimental trend in the CO frequencies for (DDQ)ⁿ is more pronounced; the frequency for the anion is ~140 cm⁻¹ less than that of the neutral species, whereas the value for the dianion is ~100 cm⁻¹ lower than that for the anion. Furthermore, the CO frequency

for the (DDQ)²⁻ in (N(C₂H₅)₄)₂⁺ (DDQ)²⁻ is at 1465 cm⁻¹, which confirms our assignment of the charge on A as -2. The decrease in frequency ν_{CO} is consistent with the decrease in the C-O bond order from two in DDQ to a nominal value of one in (DDQ)²⁻.

The scaled, calculated frequencies for the cyano groups in DDQ and (DDQ)²⁻ are presented in Table 2, as are the calculated infrared frequencies for the cyano groups in TCNQ and (TCNQ)²⁻ (24). The scaled frequencies are in good agreement with the experimental values, especially when our use of a single average scale factor is considered. As expected, the calculated frequencies for the dianions are significantly lower in energy than those for the neutral form. The large splitting of the cyano group frequencies in (TCNQ)²⁻ is an inherent property of the isolated dianion (10). For (DDQ)²⁻ we do not calculate such a splitting; thus, the observed splitting probably arises from solid-state effects. Although the calculated infrared intensities are only approximate, the lower frequency mode of the cyano groups should show intensity in the dianion that is greatly enhanced as compared to the neutral species. The calculated CO frequencies show the same dramatic shift to lower frequency for the dianion as compared to the neutral species, as was found experimentally. For DDQ the two CO stretches are predicted to be of comparable intensity. For (DDQ)²⁻ the lower frequency CO stretch is predicted to have a very small intensity; the higher frequency band is predicted to have a large intensity. This is consistent with the experimental observation of only one intense band. The splitting for the CO bands in DDQ and (DDQ)²⁻ is predicted to be small; for DDQ this is in good agreement with the data. These studies of vibrational spectra are consistent with our assignment of a value of *n* = -2 for (DDQ)ⁿ in these charge-transfer complexes.

Table 2. Infrared vibrational transitions for acceptor complexes. Abbreviations for the acceptor groups are given in (5). The neutral C₆(CN)₆ complex has not been synthesized. Experimental values are from nujol mulls. Calculated values are given in parentheses and are scaled by a factor of 0.82. The scale factor was taken from (10). Letter designations for the experimental values indicate intensity: s = strong, m = medium, w = weak.

Acceptor	Vibrational frequency (cm ⁻¹)		
	Neutral	Monoanion	Dianion
		<i>Cyano</i> , ν(C≡N)	
TCNQ	2222 m, 2226 m (2230, 2234)*	2153 m, 2179 s	2105 s, 2150 s (2107, 2160)*
TCNQF ₄	2228 s	2178 s, 2196 s	2133 s, 2167 s
TCNE	2221 m, 2259 s	2144 s, 2183 s	2069 s, 2104 s
C ₄ (CN) ₆	2238 m, 2247 s, 2253 m, 2211w	2168 m, 2185 s, 2207 w, 2220 w	2123 s, 2151 s, 2200 m
C ₆ (CN) ₆		2196 m, 2210 m	2150 s, 2197 s
DDQ	2234 w, 2246 w (2233, 2236)	2206 s	2169 m, 2192 w (2157, 2160)
		<i>Carbonyl</i> , ν(C=O)	
DDQ	1701 s, 1691 s† (1674, 1670)	1562 s, 1544 m‡	1460 s§ (1488, 1480)¶

*Data taken from (10). †Data taken from (9).

‡(Fe(C₅(CH₃)₅)₂)⁺ salt. The (N(C₂H₅)₄)⁺ salt has transitions at 1580 and 1538 cm⁻¹.

§The (N(C₂H₅)₄)⁺ salt has a CO stretch at 1465 cm⁻¹. ¶The transition at 1480 cm⁻¹ is predicted to have almost zero intensity.

REFERENCES AND NOTES

- J. S. Miller *et al.*, *Chem. Commun.* **1986**, 1026 (1986).
- J. S. Miller *et al.*, *J. Am. Chem. Soc.*, in press.
- J. S. Miller, A. J. Epstein, W. M. Reiff, *Isr. J. Chem.*, in press.
- G. A. Candela, L. Swarzenruber, J. S. Miller, M. J. Rice, *J. Am. Chem. Soc.* **101**, 2755 (1979).
- $C_4(CN)_6$ = pericyano-1,3-butadiene; $C_6(CN)_6$ = hexacyanotrimethylenecyclopropane; TCNQ = 7,7,8,8-tetracyano-*p*-quinodimethane; TCNQF₄ = perfluoro-TCNQ; DDQ = 2,3-dichloro-5,6-dicyanobenzoquinone; TCNE = tetracyanoethylene; TCNQ(CN)₄ = pericyano-TCNQ.
- J. H. Zhang, W. M. Reiff, J. S. Miller, unpublished results.
- The following crystallographic analysis was performed by Oneida Research Services; space group = $P2_1/c$; $a = 9.382 (\pm 0.004) \text{ \AA}$; $b = 11.797 (\pm 0.002) \text{ \AA}$; $c = 19.520 (\pm 0.009) \text{ \AA}$; $\beta = 98.34^\circ$; $V = 2138 (\pm 2) \text{ \AA}^3$; $Z = 2$, $R_w = 8.1\%$, where a , b , and c are the lengths and β is the angle that define the unit cell, V is the volume of the unit cell, Z is the number of molecules in the unit cell, and R_w is the weighted agreement factor. Full crystallographic data will be deposited in the Cambridge Crystallographic Database.
- D. A. Dixon, J. C. Calabrese, J. S. Miller, *J. Am. Chem. Soc.* **108**, 2582 (1986).
- J. S. Miller *et al.*, *ibid.*, p. 449.
- J. S. Miller *et al.*, unpublished results.
- D. P. Freyberg, J. L. Robbins, K. N. Raymond, J. C. Smart, *J. Am. Chem. Soc.* **92**, 892 (1971).
- The STO-3G basis set has 1s, 2s, and three 2p functions on carbon, nitrogen, and oxygen. For chlorine, there are 1s, 2s, 3s, three 2p, and three 3p functions. These are formed by contracting three Gaussian functions for each basis function as described by W. J. Hehre, R. F. Stewart, and J. A. Pople [*J. Chem. Phys.* **51**, 2657 (1969)].
- HONDO is a general ab initio molecular orbital program system as described by M. Dupuis, J. Rys, and H. F. King, [*ibid.* **65**, 111 (1965)] and H. F. King, M. Dupuis, and J. Rys [*National Resource for Computer Chemistry Software Catalog* (National Resource for Computer Chemistry, Berkeley, CA, 1980), vol. 1, program QHO2 (HONDO) (available from University of California, Berkeley)].
- GRADSCF is an ab initio gradient program system designed and written by A. Komornicki at Polyatomics Research, Mountain View, CA, and supported by grants through the NASA-Ames Research Center.
- A. Komornicki, K. Ishida, K. Morokuma, R. Ditchfield, M. Conrad, *Chem. Phys. Lett.* **45**, 595 (1977).
- P. Pulay, in *Applications of Electronic Structure Theory*, H. F. Schaefer III, Ed. (Plenum, New York, 1977), chap. 4.
- H. F. King and A. Komornicki, *J. Chem. Phys.* **84**, 5645 (1986).
- L. E. Sutton, *Tables of Interatomic Distances and Configuration in Molecule and Ions, Supplement, Special Publication No. 18* (Chemical Society, London, 1965), p. 20s.
- The C-Cl bond lengthens by 0.05 Å in (DDQ)²⁻ as compared to DDQ.
- The STO-3G basis set has 78 basis functions and the DZD basis set has 148 basis functions. The calculations scale as N^4 , where N is the number of basis functions.
- The *s* and *p* basis set for carbon, nitrogen, and oxygen is from T. H. Dunning, Jr., and P. J. Hay [in *Methods of Electronic Structure Theory*, H. F. Schaefer III, Ed. (Plenum, New York, 1977), chap. 1]. The *s* and *p* basis set for chlorine is from A. D. McLean and G. S. Chandler [*J. Chem. Phys.* **72**, 5639 (1980)].
- J. Breulet *et al.*, *J. Am. Chem. Soc.* **106**, 6250 (1984).
- D. A. Dixon and J. S. Miller, unpublished results.
- The scale factor 0.82 is taken from the ratio of v_{calc} to v_{calc} given in (10).

29 September 1986; accepted 30 December 1986

Conservation of Brain Amyloid Proteins in Aged Mammals and Humans with Alzheimer's Disease

DENNIS J. SELKOE, DOUGLAS S. BELL, MARCIA B. PODLISNY, DONALD L. PRICE, LINDA C. CORK

The formation of clusters of altered axons and dendrites surrounding extracellular deposits of amyloid filaments (neuritic plaques) is a major feature of the human brain in both aging and Alzheimer's disease. A panel of antibodies against amyloid filaments and their constituent proteins from humans with Alzheimer's disease cross-reacted with neuritic plaque and cerebrovascular amyloid deposits in five other species of aged mammals, including monkey, orangutan, polar bear, and dog. Antibodies to a 28-amino acid peptide representing the partial protein sequence of the human amyloid filaments recognized the cortical and microvascular amyloid of all of the aged mammals examined. Plaque amyloid, plaque neurites, and neuronal cell bodies in the aged animals showed no reaction with antibodies to human paired helical filaments. Thus, with age, the amyloid proteins associated with progressive cortical degeneration in Alzheimer's disease are also deposited in the brains of other mammals. Aged primates can provide biochemically relevant models for principal features of Alzheimer's disease: cerebrovascular amyloidosis and neuritic plaque formation.

ALZHEIMER'S DISEASE (AD) IS AN age-related brain degenerative disease that is the most common cause of intellectual failure in late life. The cerebral cortex of patients with AD contains intraneuronal masses of cytoplasmic filaments [neurofibrillary tangles (NFTs)] and clusters of degenerating axons and dendrites (neuritic or senile plaques) (1). In many cases, these degenerating neurites surround a core of extracellular proteinaceous filaments that have the structural and tinctorial properties of amyloid. In most cases of AD, morphologically and immunochemically identical amyloid filaments also occur in the walls of some capillaries, arterioles, and small arteries in the cerebral cortex and in some meningeal arteries (2-5). In an electron microscopic study, every neuritic plaque examined by

serial sectioning in six cases of AD contained a capillary with amyloid filaments at its basement membrane (6). Neuritic plaques and NFTs occur in abundance in AD; however, a smaller number of qualitatively identical lesions occur in restricted topographic distribution in the brains of most neurologically normal aged humans (7).

The lack of a naturally occurring analog of AD in animals has been a major obstacle to studying the pathogenesis of the disease. An animal model that shows cortical neuritic degeneration and deposition of amyloid fibers that are biochemically closely related to or the same as those in aged humans could facilitate understanding of the genesis of neuritic plaques and microvascular amyloidosis. Aged monkeys and dogs develop plaques in the cerebral cortex (8-11) that are

composed of neurites from multiple neurotransmitter systems (10-12) surrounding deposits of amyloid (8, 9). We have now shown that the amyloid in senile plaques and cerebral vessels in three species of aged nonhuman primates, in dogs, and in a polar bear cross-react with a panel of antibodies raised against human senile plaque amyloid and its constituent proteins.

We examined the brains of three rhesus monkeys (*Macaca mulatta*) (30, 31, and 31 years of age; equivalent human age ~90 years); an orangutan (*Pongo pygmaeus*) that died naturally in a zoo (46 years); two squirrel monkeys (*Saimiri sciureus*) (20 and 23 years); nine dogs (12 to 16 years) that died of natural causes; and a polar bear (*Ursus maritimus*) (28 years) that was killed by euthanasia in a zoo. Brains were fixed by immersion in 10% buffered Formalin except for one monkey, which was anesthetized and perfused with 4% paraformaldehyde. Blocks of neocortex were embedded in paraffin, and 10- to 15- μm coronal sections were cut and mounted on albuminized slides for immunocytochemistry. We used several rabbit antisera (Table 1). Two of these, designated S and V, were raised against partially purified fractions of human paired helical filaments (PHFs) prepared from cerebral cortex of patients with AD (13). Because such PHF-enriched fractions contain variable amounts of contaminating am-

D. J. Selkoe, D. S. Bell, M. B. Podlisky, Department of Neurology (Neuroscience), Harvard Medical School, and Center for Neurologic Diseases, Department of Medicine (Neurology), Brigham and Women's Hospital, Boston, MA 02115.

D. L. Price and L. C. Cork, Division of Comparative Medicine and Neuropathology Laboratory, Departments of Pathology, Neurology and Neuroscience, Johns Hopkins University School of Medicine, Baltimore, MD 21205.